Superregenerative Incoherent UWB Pulse Radar System

Thomas Wuchenauer, Martin Nalezinski and Wolfgang Menzel*
Siemens AG, Munich, Germany, Email: wuchenauer@ieee.org
*Microwave Techniques, University of Ulm, Germany

***Abstract*— A new short range ultra wideband (UWB) radar system with a very simple design due to its superregenerative receiver concept has been studied. The system does not require any amplification of RF or IF signals which allows to build a very inexpensive low-power sensor. With measurements, simple mathematical models and a simulation in time-domain the voltage amplitude of the measurement signal of the receiver is investigated. The applicability as a sensor is shown in a radar device.**

***Index Terms*— UWB, pulse radar, superregenerative receiver.**

I. INTRODUCTION

THE principle of superregenerative reception is well known since Armstrong's descriptions [1] in 1922. Today it is widely used in low cost communication systems like garage openers or wireless sensors. In the past there have been different approaches to theoretically describe superregenerative receivers [2]-[5], but only for use in communication systems.

A disadvantage of this receiver type in communication systems is the spurious emission of electromagnetic power due to the necessary operation of a pulse oscillator. An active radar system inherently requires these emissions and is therefore well suited to use a superregenerative receiver.

Section II explains the radar sensor and gives a functional description of the superregenerative receiver.

Section III gives a mathematical approach to explain the properties of a quenched and stimulated oscillator. A simulation in time-domain is done to verify the results.

Section IV shows the measured results of the receiver both as a stand-alone component and in the radar device to confirm the applicability of the system approach.

II. RADAR SYSTEM

A block diagram of the radar system is given in Fig. 1. Measurement starts with a continuous train of short TX-baseband-pulses (typ. 1 ns 6 dB-width and 5 V amplitude) coming from the pulse generator (PG) that is clocked by $\mathrm{CLK_{TX}}$ with f_{TX} (typ. 1 MHz). The pulse-train is used by the pulse oscillator (PO) to generate RF-pulses ($\mathrm{RF_{TX}}$, typ. 24 GHz and 1 GHz bandwidth) which are transmitted by the antenna after passing the power detector (PD). To detect the echo a second RF-pulse-train ($\mathrm{RF_{LO}}$) with a slightly different pulse repetition frequency $f_{\mathrm{LO}} = f_{\mathrm{TX}} + \Delta f$ from $\mathrm{CLK_{LO}}$ (typ. 1 MHz+50 Hz) is generated. If a reflected $\mathrm{RF_{TX}}$-pulse arrives at the monostatic device exactly at the moment when a subsequent LO-pulse switches on the oscillator, the resulting $\mathrm{RF_{LO}}$-pulse is stimulated and oscillates faster and stronger than without stimulation. Since the PD measures continuously the sum of $\mathrm{RF_{TX}}$ and $\mathrm{RF_{LO}}$ power it detects additional power if $\mathrm{RF_{LO}}$ is stimulated. This way the PO serves both as a transmitter and a receiver which simplifies the device compared to a traditional pulse radar device with separate transmitter and receiver paths.

The small difference Δf in frequency allows a sequential sampling that provides a low-frequency measurement signal which can be displayed on an oscilloscope triggered with a rate of Δf. The theoretical range of unambiguity $R_{\text{unambiguity}} = \frac{c_0}{2 \cdot f_{\mathrm{TX}}}$ is halved with respect to conventional radars, because there is no distinction between TX and LO path and therefore the measurement signal is symmetrical relative to the trigger edge.

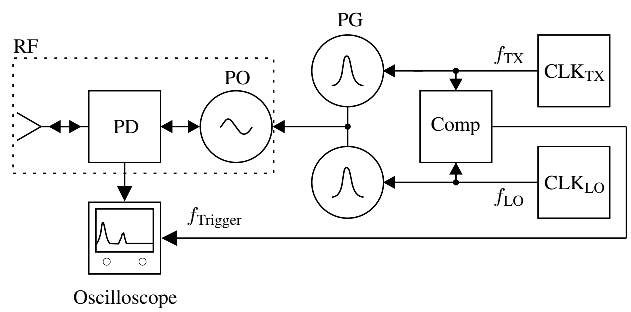

Fig. 1. Block diagram of the radar system with pulse oscillator (PO), actuating pulse generators (PG) and power detector (PD).

III. RECEIVER MODELLING

In a superregenerative receiver a periodically quenched oscillator varies the slope of its rising edge when stimulated with a signal of the same frequency as the resonance frequency. The oscillator can be modelled with an equivalent circuit diagram as given in Fig. 2. The circuit follows the well known approach to undamp the tank circuit by an amplifying device like a tube or a transistor represented by a negative resistance. The resistance $-R_n (< 0)$ in Fig. 2 is the resulting sum of loop resistance and negative resistance. In transmission mode of the radar, when no echo signal is present, the stimulation voltage U_S is zero and switch S is controlled by $\mathrm{CLK_{TX}}$. In reception mode U_S is caused by the echo of $\mathrm{RF_{TX}}$ and S is controlled by $\mathrm{CLK_{LO}}$. The latter mode is analyzed below.

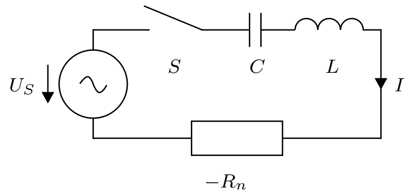

Fig. 2. Equivalent circuit diagram of the oscillator with resistance $-R_n$, switch S and stimulating voltage U_S.

Frink gives in [6] the diffential equation for the circuit in Fig. 2:

$$L\frac{dI}{dt} - R_n \cdot I + \frac{1}{C}\int I dt = U_S \tag{1}$$

or

$$LC\frac{d^2I}{dt^2} - R_nC \cdot \frac{dI}{dt} + I = \omega_S A \cdot \cos(\omega_S t) \tag{2}$$

with $U_S = A \cdot \sin(\omega_S t)$ where A is the voltage amplitude and ω_S the angular frequency of the stimulating pulse. This approach supposes a constant amplification of the transistor for all voltage amplitudes which is only an approximation during start-up time of the oscillation. However, equ. (2) is only analytically solvable for a constant function $R_n \neq f(I)$ why this simplified approach is used first and a consideration of nonlinear amplification is done in a second step.

Provided that frequency ω_S of the stimulating pulse equals the resonant frequency $\omega_0 = \frac{1}{\sqrt{LC}}$ of the tank circuit, the solution of equ. (2) is given as follows:

$$I = \frac{A\omega_0 \cdot e^{(R_n/2L)t}}{R_n\beta}\sin(\beta t) - \frac{A\sin(\omega_0 t)}{R_n} \tag{3}$$

with $\beta = \sqrt{\frac{1}{LC} - \frac{R_n^2}{4L^2}}$. The second term of equ. (3) represents a current of the steady-state which is not of interest at this point. Only the factor of the first sine-function raising exponentially versus time is important during the start-up period. It represents the envelope of the pulse slope. In most tank circuits $R^2/4L^2$ is small compared to $1/LC$, why $\beta \approx \omega_0$ can be approximated.

This way the current envelope $I_0(t)$ during start-up is given as

$$I_0(t) = \frac{A \cdot e^{(R_n/2L)t}}{R_n}. \tag{4}$$

The faster each pulse reaches its maximum current amplitude the longer it oscillates and the higher is the average signal power. The variation ΔP of the signal power is determined by the variation of oscillation time. Changing amplitude A of the stimulating signal in equ. (4) results in a earlier pulse start-up. Let A_1 be a initial amplitude which is changed to A_2 ($A_2 > A_1$). For the time shift Δt it follows

$$\Delta t = \frac{2L}{R_n}(\ln A_2 - \ln A_1) \propto \Delta P. \tag{5}$$

The power P_R of the backscattered and received $\mathrm{RF_{TX}}$ signal in a radar follows the equation

$$\frac{P_R}{P_T} \propto R^{-4} \tag{6}$$

in which P_T is the transmitted power and R the distance between device and target. Considering

$$P_R \propto A_2^2 \tag{7}$$

leads to

$$\Delta P = \kappa \cdot \frac{-4L}{R_n}\ln R - \frac{2L}{R_n}\ln A_1 \quad \text{with} \quad \kappa = \text{const.} \tag{8}$$

or shorter

$$\Delta P = -\alpha \cdot \ln R - K \quad \text{with} \quad \alpha, K = \text{const.} \tag{9}$$

Thus the approach with a constant negative resistance $-R_n$ explains the earlier raise of the oscillation, but not the steeper slope as it is observable in a real oscillator, especially at small stimulating signal amplitudes. A better understanding of the behavior will be derived by an examination of the amplitudes of oscillator current I and stimulating signal U_S.

Leenaerts presents in [7] an approach to describe the voltage amplitudes in a classical superregenerative receiver with a nonlinear tube amplifier. He states a simplified model to explain the behavior of the amplitudes during start-up in case an external stimulating voltage is applied. With a similar calculation one can see that the amplitude B of the gate-source-voltage at the transistor is connected to the amplitude A of the stimulating pulse by the nonlinear equation

$$B \propto A^{\frac{1}{3}} \tag{10}$$

Defining the sensitivity $G = \frac{dB}{dA}$ makes clear that with

$$G \propto A^{-\frac{2}{3}} \tag{11}$$

a small stimulating amplitude A experiences a large gain. So the stimulated pulse oscillates not only earlier but also with a shorter rise time.

Leenaerts calculation cannot give a analytical function of the pulse envelope. But it shows that the shorter rise time of the pulse edge is due to the nonlinear amplification which finally leads to a nonlinear sensitivity and the deviant behavior of the receiver at small stimulating voltages.

However, it is possible to calculate the start-up oscillation numerically and run a nonlinear transient simulation in time-domain. As shown in Fig. 3 a large-signal model of the transistor (AMP) is connected to a set of scattering parameters of the linear passive feedback system (LPS) using a circuit simulator [8]. Sweeping the interfering voltage amplitude U_{stim} and integrating over several RF-pulses of a 1 MHz pulse train leads to the characteristic curve of the receiver in Fig. 4 which plots the average oscillator RF-power versus $\frac{1}{\sqrt{U_{\text{stim}}}}$. The latter can be calculated by equ. (6) and equ. (7) and interpreted as distance R. The noise-like deviations increasing with U_{stim} arise from the loss of coherency and a inherent undersampling of the calculated and integrated signal due to software limitations.

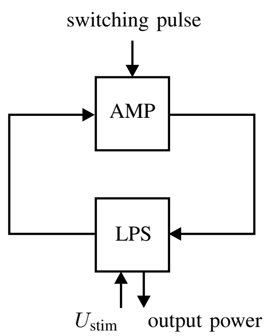

Fig. 3. Block diagram of the time-domain simulation, consisting of a large-signal model of the transistor (AMP) and a linear passive system (LPS).

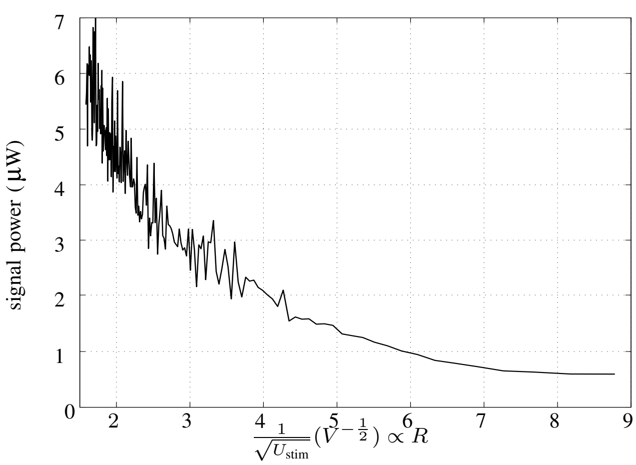

Fig. 4. Simulation of the oscillator RF-signal power versus $\frac{1}{\sqrt{U_{\text{stim}}}} \propto R$.

Fig. 5 plots the power versus $\frac{1}{\sqrt{U_{\text{stim}}}}$ on a logarithmic abscissa. Clearly visible is the linear characteristic of the curve which illustrates the logarithmic slope from Fig. 4. At small stimulating power, which equals large distances, the curve flattens as predicted by the nonlinear relation of amplitudes in equ. (10). Fig. 6 is plotted with a U^2_{stim} abscissa for comparison. The nonlinear slope illustrates that the receiver's characteristic curve does not increase linearly with U^2_{stim} ($\propto R^{-4}$) as expected from regular receivers.

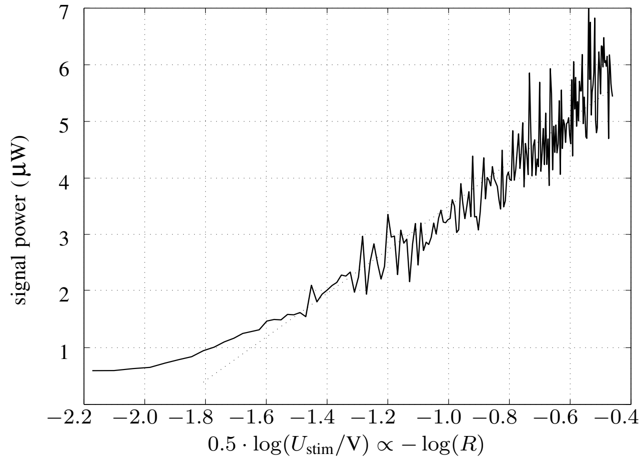

Fig. 5. Simulation of the oscillator RF-signal power (as in Fig. 4) versus a logarithmized abscissa. The dotted line serves for comparison with a linear slope.

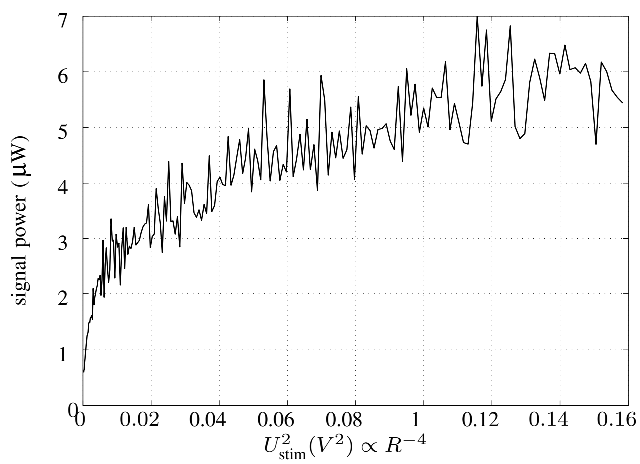

Fig. 6. Simulation of the oscillator RF-signal power (as in Fig. 4) versus a $U^2 (\propto R^{-4})$ abscissa.

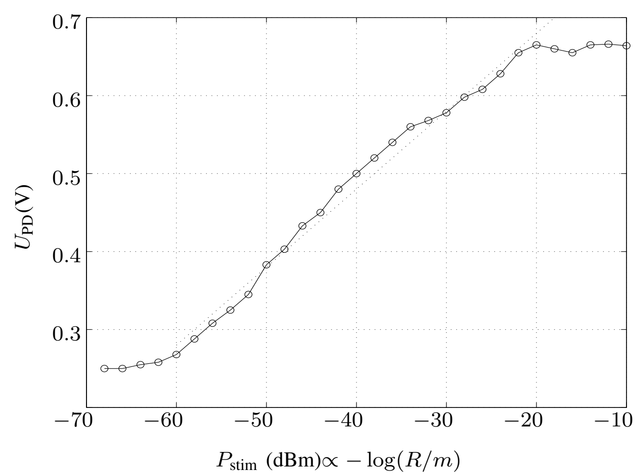

Fig. 7. Measurement of the power detector output versus $\log(P_{\text{stimu}})$. The dotted line serves for comparison with a linear slope.

IV. RESULTS

Plotting the characteristic curve of the receiver, which shows the oscillation's power versus the square root of the stimulator's power, allows to compare measured Fig. 7 with simulated Fig. 5. The power measurement is done with a power detector the output voltage U_{PD} of which is linear with the RF-signal power. The minimum sensitivity of the system is determined with -65dBm input power, which corresponds to a target distance of 25 m. Usually the sensitivity of a regular pulse radar receiver transmitting with the same RF-power is several few decibels higher, but at the cost of much higher compexity of hardware. The output signal of the complete radar device is plotted in Fig. 8. The measurement is done with a transmitted average output power of -28 dBm, 900 MHz bandwidth (3 dB) at 24 GHz, 1 MHz PRF, an antenna with 20 dB gain and a corner reflector as target with a calculated equivalent radar cross section of $0.8\,\mathrm{m}^2$. In Fig. 8 the strong peaks in the middle are caused by the antenna mismatch, the smaller peaks result from the target at a distance of 2.1 m. Clearly visible is the symmetry of the echo relative to the trigger moment (at $t = 0.2\,\mathrm{ms}$).

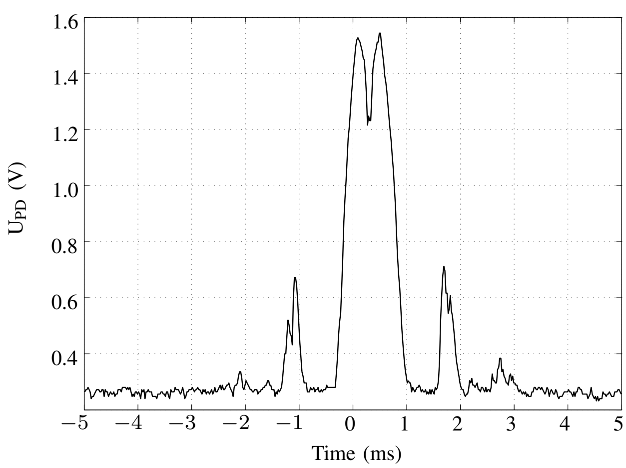

Fig. 8. Time-domain signal of the power detector of the radar device measuring a target at distance of 2.1 m. Trigger is at $t = 0.2\,ms$.

Fig. 9 shows the measured power detector output voltage versus the logarithmized distance R. This plot allows to compare the behavior of the radar system with the simulated (Fig. 5) and the measured (Fig. 7) single oscillator. All three curves illustrate that the detected signal power flattens towards large distances and increases almost linearly with $-\log(R)$.

V. CONCLUSION

The paper shows the advantageous use of a superregenerative receiver in a radar system. Due to nonlinear effects in the quenched and stimulated oscillator the sensitivity of the receiver increases with decreasing input power. The output measurement signal can be approximated with a logarithmic function of the stimulating input power. This leads to a smaller decline of the measurement signal versus target distance in a radar device compared to conventional radar systems. No additional amplification is needed in RF or in IF path. This enables a low-cost low-power device, applicable for up to several ten meters. Accuracy and resolution of the system are in accordance with regular pulse radar systems.

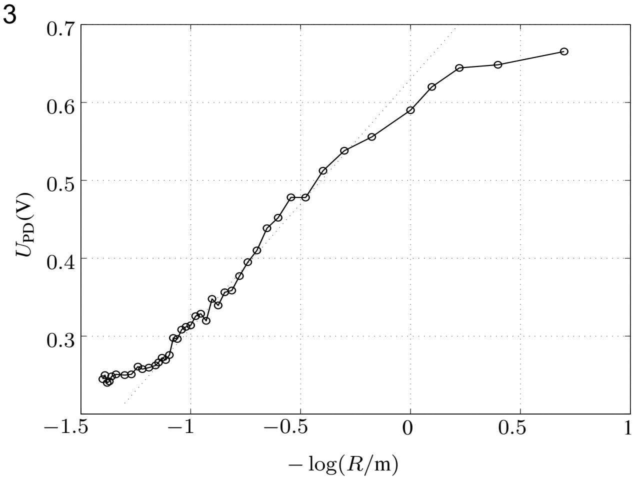

Fig. 9. Detector voltage (proportional to oscillator power) versus logarithmized distance R between 0.2 and 25m.

REFERENCES

[1] E.H. Armstrong. Some recent developments of regenerative circuits, *Proceedings of the Institute of Radio Engineers*, vol. 10, no. 8, pp. 244-260, 1922.

[2] Rodolfo Feick, Osvaldo Rojas. Modeling and simulation of the superregenerative receiver. *IEEE Transactions on Consumer Electronics*, vol. 43, no. 2, May 1997.

[3] N.B. Buchanan, V.F. Fusco, J.A.C. Stewart. A K_a-band Super Regenerative Detector. *IEEE MTT-S International Microwave Symposium Digest*, pp. 1585-1588, June 2000.

[4] N.B. Buchanan, V.F. Fusco, J.A.C. Stewart. A 7.5-GHz Super Regenerative Detector. *IEEE Transactions on Microwave Theory and Techniques*, vol. 50, no. 9, September 2002.

[5] F.X. Moncunill, P. Palà-Schönwälder, C. Dehollain, N. Joehl, M. Declerq. A 2.4-GHz DSSS Superregenerative Receiver With a Simple Delay-Locked Loop. *IEEE Microwave and Wireless Component Letters*, vol. 15, no. 8, August 2005.

[6] F.W. Frink. The Basic Priciples of Superregenerative Reception. *Proceedings of the Institute of Radio Engineers*, vol. 26, no. 1, January 1938.

[7] D.M.W. Leenaerts. Chaotic Behavior in Super Regernerative Detectors. *IEEE Transactions on Circuits and Systems-I: Fundamental Theory and Applications*, vol. 43, no.3, March 1996.

[8] Agilent Technologies. *Advanced Design System (ADS)*. Circuit Simulator.

[9] Agilent Technologies. *Momentum*. 2 1/2-D Field Simulator.